Eur. Phys. J. B **40**, 397–402 (2004)
DOI: 10.1140/epjb/e2004-00210-2

THE EUROPEAN PHYSICAL JOURNAL B

Novel phenomena in dilute electron systems in two dimensions

M.P. Sarachik[1,a] and S.V. Kravchenko[2]

[1] Physics Department, City College of the City University of New York, New York, New York 10031, USA
[2] Physics Department, Northeastern University, Boston, Massachusetts 02115, USA

Received 30 January 2004
Published online 20 July 2004 –

Abstract. Based on theory and experiments in weakly interacting electron systems, it was believed for many years that no metallic phase is possible in two dimensions. The unexpected observation of metallic-like behavior in strongly interacting electron systems has thus drawn considerable attention. Following background material and a brief history, we review the dramatic response of these 2D systems to in-plane magnetic fields, and the evidence this provides for a possible quantum phase transition.

PACS. 71.30.+h Metal-insulator transitions and other electronic transitions – 73.40.Qv Metal-insulator-semiconductor structures (including semiconductor-to-insulator) – 73.50.Jt Galvanomagnetic and other magnetotransport effects (including thermomagnetic effects)

For nearly two decades it was believed that in the absence of an external magnetic field ($B = 0$) all two-dimensional systems of electrons are insulators in the limit of zero temperature. Based on a scaling theory for non-interacting electrons [1], these expectations were further supported by theoretical work for weakly interacting electrons [2].

Confirmation of insulating behavior of two-dimensional systems of electrons in zero field was provided by a beautiful series of experiments in thin metallic films [3] and silicon MOSFETs (metal-oxide-semiconductor field-effect transistors) [4,5], where the conductivity was shown to display weak logarithmic corrections presumably leading to infinite resistivity in the limit of zero temperature. However, with the advent of higher mobility lower disorder samples which allowed access to very low electron densities, experiments in dilute silicon MOSFETs suggested that a transition from insulating to conducting behavior occurs with increasing electron density at a very low critical density, $n_c \sim 10^{11}$ cm^{-2} [6]. First viewed with considerable skepticism, the finding was soon confirmed for silicon metal-oxide-semiconductor MOSFETs fabricated in other laboratories [7], and then for other materials, including p-type SiGe structures [8] and AlAs/AlGaAs heterostructures [9], and n-type AlAs [10] and GaAs/AlGaAs heterostructures [11] (for a complete set of references, see review [12,13]).

It was soon realized that the low electron (or hole) densities for which these observations were made correspond to a regime where the energy of the repulsive Coulomb interactions between the electrons exceeds the Fermi energy by an order of magnitude or more. For example, at an electron density $n_s = 10^{11}$ cm^{-2} in silicon MOSFETs, the Coulomb repulsion energy, $U_c \sim e^2(\pi n_s)^{1/2}/\epsilon$, is about 10 meV while the Fermi energy, $E_F = \pi n_s \hbar^2/2m^*$, is only 0.55 meV. (Here e is the electronic charge, ϵ is the dielectric constant, and m^* is the effective mass of the electron.) Rather than being a small perturbation, interactions instead provide the dominant energy in these very dilute systems.

The resistivity of a high-mobility (low disorder) silicon MOSFET is shown at several fixed temperatures as a function of electron density in Figure 1a. There is a well defined crossing at a "critical" electron density, n_c, below which the resistivity increases as the temperature is decreased, and above which the reverse is true. This can be seen more clearly in Figure 1b where the resistivity is plotted as a function of temperature for various fixed electron densities. A resistivity that increases with decreasing temperature generally signals an approach to infinite resistance at $T = 0$, that is, to insulating behavior; a resistivity that decreases as the temperature is lowered is characteristic of a metal where the resistivity tends to a finite value (or a superconductor or perfect conductor if the resistivity tends to zero). Similar behavior was subsequently found in other materials at critical densities determined by material parameters such as effective masses and dielectric constants. The value of the resistivity at the transition (the "critical resistivity" ρ_c) in all cases is on the order of h/e^2, the quantum unit of resistivity.

The electrons' spins play an important role in these low-density materials, as demonstrated by the dramatic response to a magnetic field applied parallel to the plane of the two-dimensional system. We note that an in-plane

[a] e-mail: sarachik@sci.ccny.cuny.edu

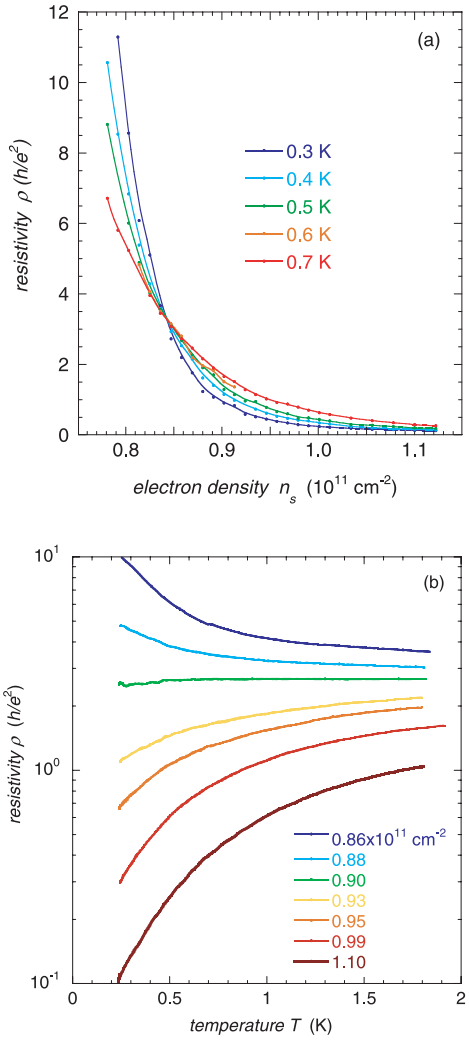

Fig. 1. (a) Resistivity as a function of electron density for the two-dimensional system of electrons in a high-mobility silicon MOSFET. The different curves correspond to different temperatures. Note that at low densities the resistivity increases with decreasing temperature (insulating behavior), while the reverse is true for higher densities (metallic behavior). (b) Resistivity as a function of temperature for the two-dimensional system of electrons in a silicon MOSFET. Different curves are for different electron densities.

magnetic field couples only to the electron spins and does not affect their orbital motion. The parallel-field magnetoresistance is shown for a silicon MOSFET in Figure 2 for electron densities spanning the density n_c at a temperature of 0.3 K. The resistivity increases by more than an order of magnitude with increasing field, saturating to a new value in fields above 2 or 3 tesla [14,15]. The total change in resistance is larger at lower temperatures and for higher mobility samples, reaching many orders of magnitude at very low temperatures for densities near n_c. Measurements of Shubnikov-de Haas oscillations have established that the saturation of the resistivity corresponds at high electron densities to full polarization of the spins [16,17]. As the density is reduced toward n_c, however, disorder and tail states play an increasingly important role [18]).

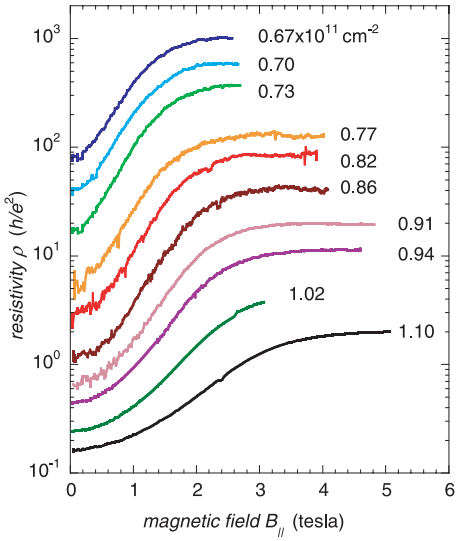

Fig. 2. For different electron densities, the resistivity at 0.3 Kelvin is plotted as a function of magnetic field applied parallel to the plane of the two-dimensional system of electrons in a silicon MOSFET. The top three curves are insulating while the lower curves are metallic in the absence of a magnetic field.

There has been much debate regarding whether the physics of strongly interacting electrons can be explained by extending Fermi liquid theory, or whether the unusual behavior of dilute two-dimensional electron systems signals new phenomena and perhaps new phases. Working within Fermi liquid theory, Zala et al. [19] have recently shown that strong interactions have a pronounced effect and can account for the behavior of dilute systems for densities down to about $1.5\,n_c$ in a restricted range of temperature. However, the theory is not applicable at lower densities approaching n_c. In the remainder of this paper, we review recent magnetoconductance data obtained for silicon MOSFETs that indicate that the magnetic susceptibility diverges at a finite density n_0 near or equal to n_c, and that the divergence of the susceptibility is due to an increase of the effective mass, while the g-factor remains essentially constant. We suggest that these results provide evidence that the system approaches a zero-temperature quantum phase transition.

There have been many attempts to obtain a quantitative measure of the strength of the response of dilute 2D systems to an external field applied parallel to the electron plane. Attempts to scale the magnetoresistance curves at different densities and temperatures have generally yielded a collapse onto a single curve at either low or high magnetic field; over a wide range of temperatures but only at the metal-insulator transition; or in a wide range of carrier densities, but only in the limit of very low temperatures. Two different scaling procedures have recently been applied successfully; although they yield results that differ somewhat in detail, the major conclusions are essentially the same.

Vitkalov et al. [20] have obtained an excellent collapse of magnetoconductivity data over a broad range of electron densities and temperatures using a single scaling parameter. Here the magnetoconductivity was

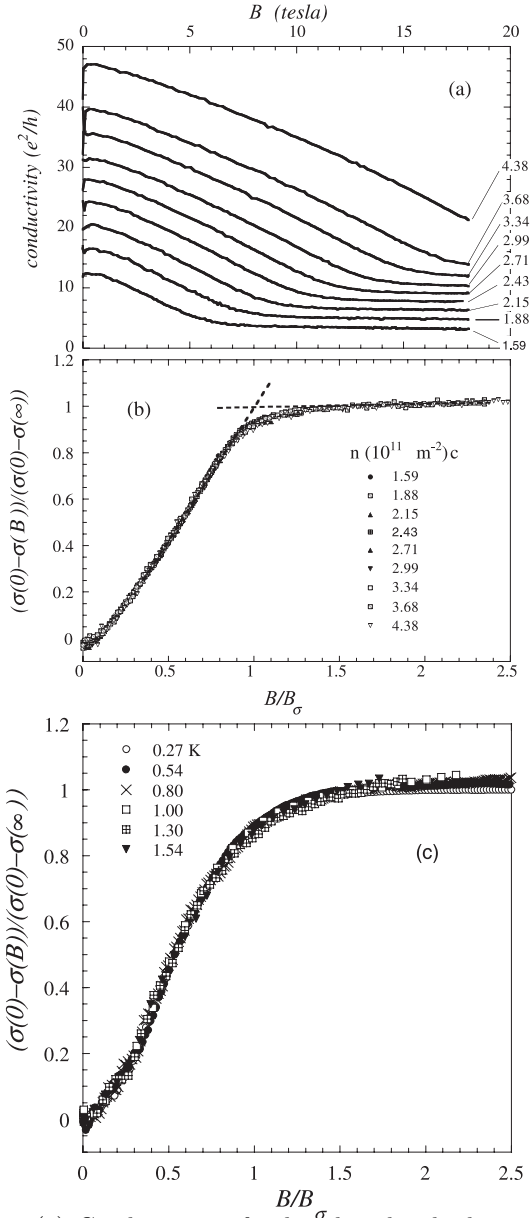

Fig. 3. (a) Conductivity of a low-disordered silicon sample versus in-plane magnetic field at different electron densities in units of 10^{11} cm^{-2}, as labeled; $T = 100$ mK. (b) Data collapse obtained by applying the scaling procedure described in the text to the curves shown in (a). (c) Data collapse obtained by applying the scaling procedure to the magnetoconductivity at different temperatures for electron density $n_s = 9.4 \times 10^{10}$ cm^{-2}.

separated into a field-dependent contribution, $(\sigma(B_\parallel) - \sigma(\infty))$, and a contribution that is independent of magnetic field, $\sigma(\infty)$. The field-dependent contribution to the conductivity, $(\sigma(0) - \sigma(B_\parallel))$, normalized to its full value, $(\sigma(0) - \sigma(\infty))$, was shown to be a universal function of B/B_σ:

$$\frac{\sigma(0) - \sigma(B_\parallel)}{\sigma(0) - \sigma(\infty)} = F(B_\parallel / B_\sigma) \qquad (1)$$

where $B_\sigma(n_s, T)$ is the scaling parameter. Applied to the magnetoconductance curves shown in Figure 3a for different electron densities above the metal-insulator transition, this procedure yields the data collapse shown in Figure 3b. Scaling also holds for the magnetoconductance at different temperatures, as illustrated in Figure 3c. The scaling holds for temperatures up to 1.6 K over a broad range of electron densities up to $4\,n_c$.

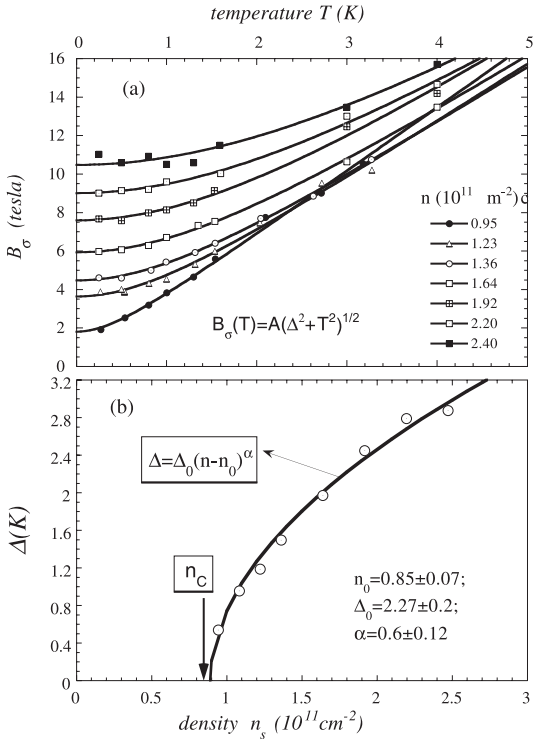

Fig. 4. (a) B_σ versus temperature for different electron-densities; the solid lines are fits to the empirical expression $B_\sigma(n_s, T) = A(n_s)[[\Delta(n_s)]^2 + T^2]^{1/2}$. (b) The parameter Δ as a function of electron density; the solid line is a fit to the critical form $\Delta = \Delta_0(n_s - n_0)^\alpha$.

Figure 4a shows the scaling parameter B_σ plotted as a function of temperature for different electron densities $n_s > n_c$. For a given density, B_σ decreases as the temperature decreases and approaches a value that is independent of temperature, $B_\sigma(T = 0)$. As the density is reduced toward n_c, the temperature dependence of B_σ dominates over a broader range and becomes stronger, and the low-temperature asymptotic value becomes smaller. Note that for electron densities below 1.36×10^{11} cm^{-2}, B_σ is approximately linear with temperature at high T. The behavior of the scaling parameter $B_\sigma(T)$ can be approximated by an empirical fitting function:

$$B_\sigma(n_s, T) = A(n_s)[\Delta(n_s)^2 + T^2]^{1/2}.$$

The solid lines in Figure 4a are fits to this expression using $A(n_s)$ and $\Delta(n_s)$ as fitting parameters. As can be inferred from the slopes of the curves of Figure 4a, the parameter $A(n_s)$ is constant over most of the range and then exhibits a small increase (less than 20%) at lower densities. As shown in Figure 4b, the parameter Δ decreases sharply with decreasing density and extrapolates to zero

at a density n_0 that is within 10% of the critical density $n_c \approx 0.85 \times 10^{11}$ cm^{-2} for the metal-insulator transition.

Using a different procedure, Shashkin et al. [21] scaled the magnetoresistivity in the spirit of the theory of Dolgopolov and Gold [22], who predicted that at $T = 0$ the normalized magnetoresistance is a universal function of the degree of spin polarization, $\xi \equiv g^*\mu_B B_\parallel/2E_F = g^*m^*\mu_B B_\parallel/\pi\hbar^2 n_s$ (here m^* is the effective mass and g^* is the g-factor). Using data at very low temperatures, where the magnetoresistance is temperature-independent and has reached its zero-temperature limit, these authors obtained a collapse of the normalized magnetoresistance, $\rho(B_\parallel)/\rho(0)$ as a function of $B_\parallel/B_c$ (here B_c is the scaling parameter normalized to correspond to the magnetic field $B_{\rm sat}$ at which the magnetoresistance saturates).

This is illustrated in Figure 5a, which shows the normalized magnetoresistance measured at different electron densities versus $B_\parallel/B_c$. The scaling is of high quality for $B_\parallel/B_c \leq 0.7$ in the electron density range 1.08×10^{11} to 10×10^{11} cm^{-2} and breaks down as one approaches the metal-insulator transition, where the magnetoresistance becomes strongly temperature-dependent even at the lowest experimentally achievable temperatures. As shown in Figure 6, the scaling parameter $B_c \propto (n_s - n_c)$ over a wide range of densities.

The two procedures yield very similar results. The scaling parameters Δ of Vitkalov et al. [20] and B_c of Shashkin et al. [21] represent energy scales $k_B\Delta$ and $\mu_B B_c$, respectively, which vanish at or near the critical electron density for the metal-insulator transition. At high electron densities and low temperatures $T < \mu_B B_c/k_B$ (corresponding to $T < \Delta$), the system is in the zero temperature limit. As one approaches n_c, progressively lower temperatures are required to reach the zero temperature limit. At $n_s = n_0$, the energies $\mu_B B_c$ and $k_B\Delta$ vanish; the parameter $B_\sigma \to 0$ as $T \to 0$; the system thus exhibits critical behavior [23], signaling the approach to a new phase in the limit $T = 0$ at a critical density $n_0 \approx n_c$.

The data obtained in these experiments provide information from which the spin susceptibility, χ, can be calculated in a wide range of densities. In the clean limit, the band tails can be neglected [18,24], and the magnetic field required to fully polarize the spins is given by the equation $g^*\mu_B B_c = 2E_F = \pi\hbar^2 n_s/m^*$ (here, the two-fold valley degeneracy in silicon has been taken into account). Therefore, the spin susceptibility, normalized by its "non-interacting" value, is

$$\frac{\chi}{\chi_0} = \frac{g^*m^*}{g_0 m_b} = \frac{\pi\hbar^2 n_s}{2\mu_B B_c m_b}.$$

The above expression yields the normalized spin susceptibility [21] and its inverse [20] shown in Figure 7. The values deduced by both groups indicate that g^*m^* diverges ($(g^*m^*)^{-1}$ extrapolates to zero) in silicon MOSFETs at a finite density close or equal to n_c. Also shown on the same figure are the data of Pudalov et al. [25] obtained from an analysis of Shubnikov-de Haas (SdH) measurements in crossed magnetic fields. The susceptibilities obtained by all three groups on different samples,

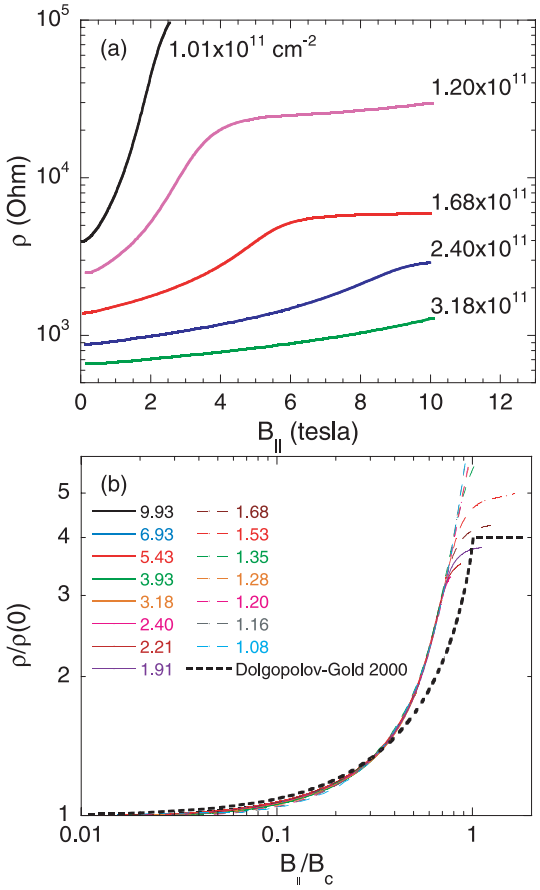

Fig. 5. (a) Low-temperature magnetoresistance of a clean silicon MOSFET in parallel magnetic field at different electron densities above n_c. (b) Scaled curves of the normalized magnetoresistance versus $B_\parallel/B_c$. The electron densities are indicated in units of 10^{11} cm^{-2}. Also shown by a thick dashed line is the normalized magnetoresistance calculated by Dolgopolov and Gold [22].

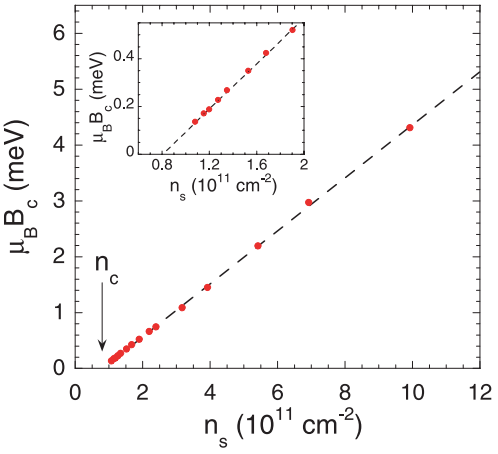

Fig. 6. Scaling parameter B_c (corresponding to the field required for full spin polarization) as a function of the electron density. An expanded view of the region near n_c is displayed in the inset.

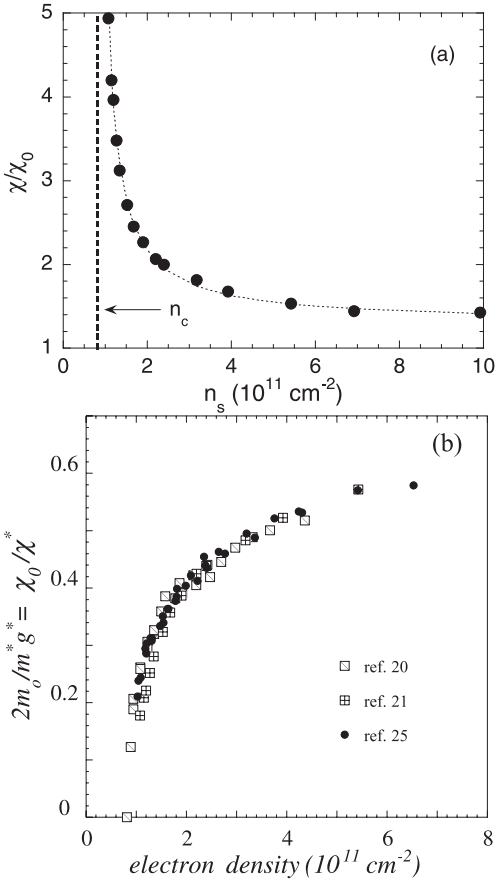

Fig. 7. (a) Normalized spin susceptibility vs. n_s. The dashed line is a guide to the eye. The vertical dashed line denotes the position of the critical density for the metal-insulator transition. (b) The inverse of the normalized spin susceptibility χ_0/χ^* versus electron density obtained by three groups, as labeled.

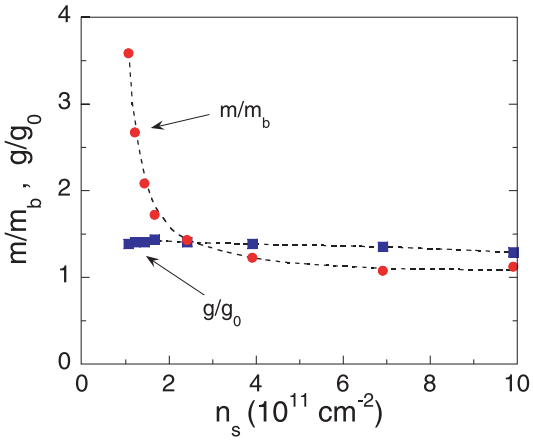

Fig. 8. The effective mass (circles) and g factor (squares) in a silicon MOSFET, determined from the analysis of the parallel field magnetoresistance and temperature-dependent conductivity, versus electron density. The dashed lines are guides to the eye.

by different methods and in different ranges of magnetic field, are remarkably similar (on the mutual consistency of the data obtained on different samples by different groups, see also Sarachik and Vitkalov [18] and Kravchenko et al. [26]).

The increase of the spin susceptibility could be due to an enhancement of either g^* or m^* (or both). Shashkin et al. [27] have obtained g^* and m^* separately by analyzing the temperature dependence of the conductivity in zero magnetic field using the recent theory of Zala et al. [19]. Values of g^*/g_0 and m^*/m_b determined from their analysis are shown as a function of the electron density in Figure 8. In the high n_s region (relatively weak interactions), the enhancement of both g and m is relatively small, both values increasing slightly with decreasing electron density in agreement with earlier data [28]. Also, the renormalization of the g-factor is dominant compared to that of the effective mass, consistent with theoretical studies [29–31]. In contrast, the renormalization at low n_s (near the critical region), where $r_s \gg 1$, is striking. As the electron density is decreased, the renormalization of the effective mass increases markedly with decreasing density while the g factor remains relatively constant. Hence, this analysis indicates that it is the effective mass, rather than the g-factor, that is responsible for the strongly enhanced spin susceptibility near the metal-insulator transition. This conclusions was verified by Shashkin et al. in reference [34], who determined the effective mass through an analysis of the temperature dependence of the SdH oscillations similar to the analysis done by Smith and Stiles [32] and Pudalov et al. [33]. By introducing a parallel magnetic field component to align the electrons' spins, Shashkin et al. [34] further demonstrated that the effective mass does not depend on the degree of spin polarization, so that the mass enhancement has no relation to the electrons' spins and exchange effects.

As discussed earlier, the divergence of the susceptibility $\chi \propto g^* m^*$ at a finite density indicates that the system is approaching a quantum phase transition to a new low-density phase. This is also supported by experiments that report a diverging compressibility [35] at or near the critical density that signals a transition between metallic and insulating behavior. The divergence of the susceptibility is associated with a diverging effective mass m^*, similar to the effective mass divergence that occurs in the He-3 system [36]. The nature of the low density phase in silicon MOSFETs is not clear at this point. The effective mass divergence could signal localization due to a Mott-type transition, or a precursor to Wigner crystallization, or perhaps a charge density wave transition. Substantial progress is being made that may soon lead to a better understanding of the interesting behavior of strongly interacting electron systems in two dimensions.

M.P. Sarachik thanks the US Department of Energy for support under grant No. DE-FG02-84-ER45153 and NSF for support under grant DMR-0129581. S.V. Kravchenko acknowledges support by NSF grant DMR-0403026 and the Sloan Foundation.

References

1. E. Abrahams, P.W. Anderson, D.C. Licciardello, T.V. Ramakrishnan, Phys. Rev. Lett. **42**, 673 (1979)
2. B.L. Altshuler, A.G. Aronov, P.A. Lee, Phys. Rev. Lett. **44**, 1288 (1980)
3. G.J. Dolan, D.D. Osheroff, Phys. Rev. Lett. **43**, 721 (1979)
4. D.J. Bishop, D.C. Tsui, R.C. Dynes, Phys. Rev. Lett. **44**, 1153 (1980)
5. M.J. Uren, R.A. Davies, M. Pepper, J. Phys. C **13**, L985 (1980)
6. S.V. Kravchenko, G.V. Kravchenko, J.E. Furneaux, V.M. Pudalov, M. D'Iorio, Phys. Rev. B **50**, 8039 (1994); S.V. Kravchenko, W.E. Mason, G.E. Bowker, J.E. Furneaux, V.M. Pudalov, M. D'Iorio, Phys. Rev. B **51**, 7038 (1995); S.V. Kravchenko, D. Simonian, M.P. Sarachik, V.M. Pudalov, Phys. Rev. Lett. **77**, 4938 (1996)
7. D. Popovic, A.B. Fowler, S. Washburn, Phys. Rev. Lett. **79**, 1543 (1997)
8. P.T. Coleridge, R.L. Williams, Y. Feng, P. Zawadzki, Phys. Rev. B **56**, R12764 (1997)
9. Y. Hanein, U. Meirav, D. Shahar, C.C. Li, D.C. Tsui, H. Shtrikman, Phys. Rev. Lett. **80**, 1288 (1998)
10. S.J. Papadakis, M. Shayegan, Phys. Rev. B **57**, R15068 (1998)
11. Y. Hanein, D. Shahar, J. Yoon, C.C. Li, D.C. Tsui, H. Shtrikman, Phys. Rev. B **58**, R13338 (1998)
12. E. Abrahams, S.V. Kravchenko, M.P. Sarachik, Rev. Mod. Phys. **73**, 251 (2001)
13. S.V. Kravchenko, M.P. Sarachik, Rep. Prog. Phys. **67**, 1 (2004)
14. D. Simonian, S.V. Kravchenko, M.P. Sarachik, V.M. Pudalov, Phys. Rev. Lett. **79**, 2304 (1997)
15. V.M. Pudalov, G. Brunthaler, A. Prinz, G. Bauer, JETP Lett. **65**, 932 (1997)
16. T. Okamoto, K. Hosoya, S. Kawaji, A. Yagi, Phys. Rev. Lett. **82**, 3875 (1999)
17. S.A. Vitkalov, H. Zheng, K.M. Mertes, M.P. Sarachik, T.M. Klapwijk, Phys. Rev. Lett. **85**, 2164 (2000); S.A. Vitkalov, M.P. Sarachik, T.M. Klapwijk, Phys. Rev. B **64**, 073101 (2001)
18. S.A. Vitkalov, M.P. Sarachik, T.M. Klapwijk, Phys. Rev. B **65**, 201106(R) (2002); M.P. Sarachik, S.A. Vitkalov, J. Phys. Soc. Jpn Suppl. A **72**, 57 (2003)
19. G. Zala, B.N. Narozhny, I.L. Aleiner, Phys. Rev. B **64**, 214204 (2001); G. Zala, B.N. Narozhny, I.L. Aleiner, Phys. Rev. B **65**, 020201(R) (2002)
20. S.A. Vitkalov, H. Zheng, K.M. Mertes, M.P. Sarachik, T.M. Klapwijk, Phys. Rev. Lett. **87**, 086401 (2001)
21. A.A. Shashkin, S.V. Kravchenko, V.T. Dolgopolov, T.M. Klapwijk, Phys. Rev. Lett. **87**, 086801 (2001)
22. V.T. Dolgopolov, A. Gold, JETP Lett. **71**, 27 (2000)
23. S.L. Sondhi, S.M. Girvin, J.P. Carini, D. Shahar, Rev. Mod. Phys. **69**, 315 (1997)
24. V.T. Dolgopolov, A. Gold, Phys. Rev. Lett. **89**, 129701 (2002); A. Gold, V.T. Dolgopolov, J. Phys.: Condens. Matter **14**, 7091 (2002)
25. V.M. Pudalov, M.E. Gershenson, H. Kojima, N. Butch, E.M. Dizhur, G. Brunthaler, A. Prinz, G. Bauer, Phys. Rev. Lett. **88**, 196404 (2002)
26. S.V. Kravchenko, A.A. Shashkin, V.T. Dolgopolov, Phys. Rev. Lett. **89**, 219701 (2002)
27. A.A. Shashkin, S.V. Kravchenko, V.T. Dolgopolov, T.M. Klapwijk, Phys. Rev. B **66**, 073303 (2002)
28. T. Ando, A.B. Fowler, F. Stern, Rev. Mod. Phys. **54**, 437 (1982)
29. N. Iwamoto, Phys. Rev. B **43**, 2174 (1991)
30. Y. Kwon, D.M. Ceperley, R.M. Martin, Phys. Rev. B **50**, 1684 (1994)
31. G.-H. Chen, M.E. Raikh, Phys. Rev. B **60**, 4826 (1999)
32. J.L. Smith, P.J. Stiles, Phys. Rev. Lett. **29**, 102 (1972)
33. V.M. Pudalov, M.E. Gershenson, H. Kojima, N. Butch, E.M. Dizhur, G. Brunthaler, A. Prinz, G. Bauer, Phys. Rev. Lett. **88**, 196404 (2002)
34. A.A. Shashkin, M. Rahimi, S. Anissimova, S.V. Kravchenko, V.T. Dolgopolov, T.M. Klapwijk, Phys. Rev. Lett. **91**, 046403 (2003)
35. S.C. Dultz, H.W. Jiang, Phys. Rev. Lett. **84**, 4869 (2000)
36. B. Spivak, Phys. Rev. B **64**, 085317 (2001); B. Spivak, Phys. Rev. B **67**, 125205 (2002)